Inorganic Chemistry

Communication

pubs.acs.org/IC

Synthesis and Structure Determination of a New Au_{20} Nanocluster Protected by Tripodal Tetraphosphine Ligands

Jing Chen, Qian-Fan Zhang, Paul G. Williard, and Lai-Sheng Wang*

Department of Chemistry, Brown University, Providence, Rhode Island 02912, United States

Supporting Information

ABSTRACT: We report the synthesis and structure determination of a new Au_{20} nanocluster coordinated by four tripodal tetraphosphine (PP_3) ligands {PP_3 = tris[2-(diphenylphosphino)ethyl]phosphine}. Single-crystal X-ray crystallography and electrospray ionization mass spectrometry show that the cluster assembly can be formulated as $[Au_{20}(PP_3)_4]Cl_4$. The Au_{20} cluster consists of an icosahedral Au_{13} core and a seven-Au-atom partial outer shell arranged in a local C_3 symmetry. One PP_3 ligand coordinates to four Au atoms in the outer shell, while the other three PP_3 ligands coordinate to one Au atom from the outer shell and three Au atoms from the surface of the Au_{13} core, giving rise to an overall chiral 16-electron Au cluster core with C_3 symmetry.

Gold (Au) nanoparticles have been found to be capable of catalyzing a variety of reactions, such as selective oxidation and hydrogenation.[1−3] However, because traditional methods of catalyst preparation usually produce a distribution of nanoparticles with a range of sizes and structures, the observed catalytic properties reflect only an average of the nanoparticle ensemble. The polydispersity of Au nanoparticles in terms of both the size and structure precludes correlation of the catalytic properties with the nanoparticle structure and electronic properties. In order to understand the origin of the catalytic properties of nanogold, it is critical to first obtain uniform atomically defined Au nanoparticles in large quantities. Over the past few years, a number of thiolate-protected Au nanoclusters with sizes larger than 10 Au atoms have been reported.[4−20] However, many fewer phosphine-protected Au nanoclusters with sizes larger than 10 Au atoms are known,[21−25] except the well-characterized undecagold Au_{11} cluster and the icosahedral Au_{13} cluster coordinated by phosphine and halide ligands.[26,27] Recently, a phosphine-coordinated Au_{20} cluster was reported, which is composed of two edge-shared Au_{11} units.[28] An Au_{14} cluster coordinated by phosphine/NO_3^- ligands[29] has also been synthesized and characterized by X-ray crystallography recently. Diphosphine-protected Au_{13} icosahedral clusters and other smaller Au clusters have also been reported.[26,27,30,31]

A tetrahedral Au_{20} cluster was found previously by the Wang group to be highly stable in the gas phase with all 20 Au atoms on the cluster surface.[32] Our preliminary studies showed that it could be stabilized by four phosphine ligands in solution,[33] leaving 16 uncoordinated surface sites. The Wang group has been pursuing the synthesis of this highly stable tetrahedral Au_{20} cluster in solution using different diphospine ligands.[34] The goal was to create atom-precise phosphine-protected Au nanoclusters with uncoordinated surface sites as potentially in situ catalytic sites without any postsynthetic treatments. Recently, we reported the crystal structure of a $Au_{22}(L^8)_6$ cluster [L^8 = 1,8-bis(diphenylphosphino)octane].[35] The Au_{22} cluster core consists of two Au_{11} units and contains eight uncoordinated surface Au atoms. The eight uncoordinated surface Au atoms in the $Au_{22}(L^8)_6$ nanocluster are unprecedented in atom-precise Au nanoparticles and can be considered as potential in situ active sites for catalysis.

Herein we extend our effort to synthesize the pyramidal Au_{20} cluster by the tripodal tetraphosphine ligand. We have indeed achieved a Au cluster composed of 20 atoms, which is coordinated by four tripodal tetraphosphine ligands with four Cl atoms as the counterions. We abbreviate this new cluster as $[Au_{20}(PP_3)_4]Cl_4$, where PP_3 = tris[2-(diphenylphosphino)-ethyl]phosphine. Although this Au_{20} cluster is not the intended tetrahedral pyramid, it does represent a highly interesting structure with unprecedented surface coordination. The Au_{20} nanocluster consists of an icosahedral Au_{13} core with a partial seven-Au-atom outer shell arranged in a tripodal shape with local C_3 symmetry. One PP_3 ligand is coordinated to four Au atoms of the outer shell, whereas the remaining three PP_3 ligands coordinate to one Au atom each in the outer shell and three Au atoms of the Au_{13} core.

Details of the synthesis are provided in the Supporting Information (SI). Briefly, the starting reagent for the synthesis was $Au_4(PP_3)Cl_4$, prepared according to Balch and Fung.[36] A dichloromethane solution of $Au_4(PP_3)Cl_4$ was reduced by $NaBH_4$ at 50 °C. The product was purified by a dichloromethane/toluene mixed solution and then used to grow single crystals suitable for X-ray analyses with a high yield [48% on the basis of the initial amount of Au in $Au_4(PP_3)Cl_4$], which was performed at the Advanced Light Source at Lawrence Berkeley National Laboratory (see the SI). The new cluster was found to be an Au_{20} core and four PP_3 ligands with the Cl^- counterions, although the Cl^- ions were somewhat disordered. The total crystal structure of $[Au_{20}(PP_3)_4]Cl_4$, shown in Figure 1,[37] was found to have an orthorhombic space group *Pbca* (see the SI). The four Cl^- counterions were independently confirmed by composition analyses (see the SI), and the charge state of $[Au_{20}(PP_3)_4]^{4+}$ was confirmed by electrospray ionization mass spectrometry (ESI-MS) spectra (vide infra). This new Au_{20} cluster is quite stable, as revealed by UV−vis spectra, and no decomposition was observed after its solution had been stored

Received: March 13, 2014
Published: March 31, 2014

   dx.doi.org/10.1021/ic500562r | *Inorg. Chem.* 2014, 53, 3932−3934

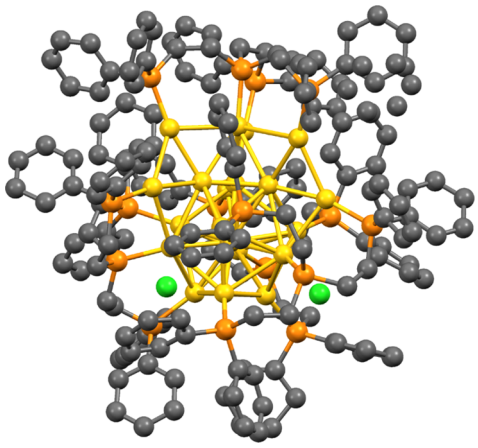

Figure 1. Total structure of $Au_{20}(PP_3)_4Cl_4$. Color labels: golden, Au; orange, P; gray, C; green, Cl. H atoms are omitted.

under ambient conditions for 2 weeks or heated at 80 °C for 1 day. The total number of valence electrons of $[Au_{20}(PP_3)_4]^{4+}$ is calculated to be 16, which does not match a case of shell closure.[11,38,39] A number of stable Au clusters have been reported recently,[29] which do not have electron counts matching a shell closure, including our recent Au_{22} nanocluster.[34]

The details of the Au core of $[Au_{20}(PP_3)_4]Cl_4$ are shown in Figure 2. The Au_{20} cluster is based on a slightly distorted

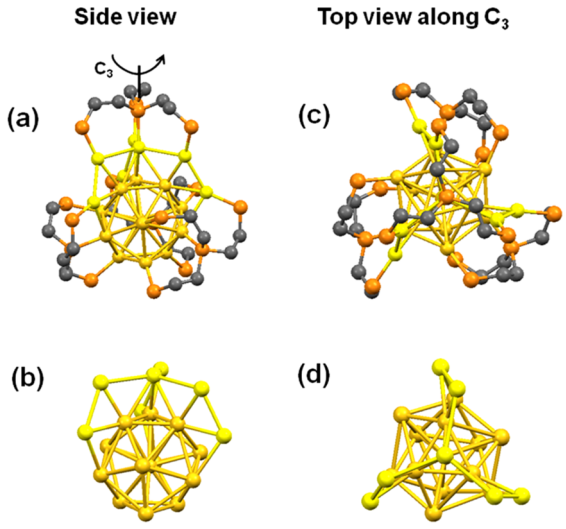

Figure 2. Details of the core structure of $[Au_{20}(PP_3)_4]Cl_4$: (a and b) side views; (c and d) top views. Color labels: golden and yellow, Au; orange, P; gray, C. Phenyl groups and H atoms are omitted.

icosahedral Au_{13} core (golden atoms), capped by a Au clamp composed of the remaining seven Au atoms (yellow atoms). The Au_{13} core possesses C_3 and C_2 rotation axes. Parts a and b of Figure 2 show two views along the C_3 axis. The Au_{13} core is composed of a top and a bottom Au_3 face, as well as a chaired Au_6 ring between the two Au_3 faces. The overall cluster dimension is about 1.1 nm if a 1.5 Å covalent radius is taken for Au atoms. The coordination environment of the Au_{20} core is highly unique, as shown more clearly in Figure 2a. Four Au atoms on the outer Au_7 clamp unit are coordinated by one PP_3 ligand, while the remaining three terminal Au atoms on the clamp share the other three PP_3 ligands with the Au_{13} core. The three Au atoms at the top Au_3 face of the Au_{13} core are not coordinated by the ligands. Figure 1 shows that the ligand protection shell is somewhat loose, so the three uncoordinated Au atoms are relatively exposed and may be considered as catalytic active sites.

The Au_{20} core adopts C_3 symmetry. The top view of the Au_{20} core along the C_3 axis is shown in Figure 2d. The arrangement of the three arms of the Au_7 clamp makes the whole cluster chiral. If the PP_3 ligands are taken into consideration, as shown in Figure 2c, the structure resembles a triblade fan with a C_3 principal axis.

It is interesting to note that the current $[Au_{20}(PP_3)_4]Cl_4$ cluster is totally different from the previous $[Au_{20}(PPhpy_2)_{10}Cl_4]Cl_2$ cluster,[28] which consists of two Au_{11} units sharing a square face. A comparison of our Au_{20} core and the Au_{13} cluster[31] is given in Figure S6 in the SI, and the detailed Au−Au distances of Au_{20} and Au_{13} are given in Table S1 in the SI. The Au_{13} unit in Au_{20} has some distortions compared with the Au_{13} core because of coordination of the PP_3 ligands. For example, the Au−Au bonds of the top Au_3 surface (Au_7−Au_8−Au_{12}) in Au_{20} are shorter than those of the top Au_3 surface of Au_{13}. This distortion is induced because of the pull of the Au_7 clamp. Furthermore, three Au atoms on the chaired Au_6 ring of the Au_{13} unit in the Au_{20} core (Au_2, Au_9, and Au_{11}) are pulled toward the PP_3 ligands.

The distortions of the Au_{13} unit in the Au_{20} core suggest that the Au_{20} core cannot have perfect C_3 symmetry. This result is reflected in the ^{31}P NMR of the $[Au_{20}(PP_3)_4]Cl_4$ cluster, as shown in Figure S3 in the SI. All of the chemical shifts in this spectrum can be assigned. The two peaks around 63 ppm and the four peaks around 48 ppm are assigned to the chemical shifts of the PP_3 ligand coordinated to the Au_7 clamp. The splitting of the peaks is induced by coupling of the phosphor atoms, which is the same as that in the pure PP_3 ligand (Figure S1 in the SI). The peaks at 54, 40, and 38 ppm are assigned to the three PP_3 ligands coordinated to the Au_{13} unit. The peaks at 38 and 40 ppm are produced by the imperfect C_3 symmetry because of distortion of the Au_{13} unit. These assignments are confirmed by the temperature-dependent ^{31}P NMR of $[Au_{20}(PP_3)_4]Cl_4$ in CD_3OD, as shown in Figure S4 in the SI. We observed that, upon increasing the temperature from 293 to 353 K, the intensity of the peak at 37 ppm is decreased at the same time that the intensity of the peak at 39 ppm is increased. The intensities of these two peaks are recovered as the temperature is cooled to 293 K, indicating that the increasing dynamic behavior of the Au_{20} core induced the asymmetry at higher temperatures.

Further characterization of the new Au_{20} cluster was carried out using ESI-MS in the positive ion mode, as shown in Figure 3. The intense peak at m/z 1655 corresponds to $[Au_{20}(PP_3)_4]^{4+}$, consistent with our X-ray structural analyses. In addition, a weak Cl^- adduct, $[Au_{20}(PP_3)_4Cl]^{3+}$, and a weakly oxidized $[Au_{20}(PP_3)_4]^{5+}$ signal were also observed. The observed isotopic pattern agrees with the simulation (Figure 3b).

The UV−vis absorption spectrum of the Au_{20} cluster in dichloromethane is shown in Figure S7 in the SI, exhibiting two prominent bands at 486 and 360 nm. The typical absorption bands of the Au_{13} cluster are located at 360 and 490 nm.[31] Figure S8 in the SI compares the optical absorption spectrum of the Au_{20} cluster with that of Au_{13} in dichloromethane.

In conclusion, we report the synthesis of a new Au_{20} nanocluster coordinated by four tripodal tetraphosphine phosphine ligands (PP_3 = Tris[2-(diphenylphosphino)ethyl]-phosphine); its formula and structure were determined to be $[Au_{20}(PP_3)_4]Cl_4$ by X-ray crystallography and ESI-MS. This new Au_{20} cluster is chiral with a local C_3 axis. The Au_{20} core is capped

dx.doi.org/10.1021/ic500562r | Inorg. Chem. 2014, 53, 3932−3934

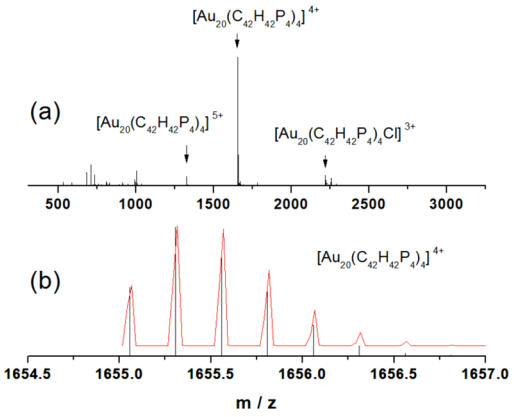

Figure 3. (a) Mass spectrum of the $[Au_{20}(PP_3)_4]Cl_4$ cluster. (b) Comparison of the measured (black tace) and simulated (red trace) isotopic patterns of $[Au_{20}(C_{42}H_{42}P_4)_4]^{4+}$.

by a relatively loose phosphine protection shell with three uncoordinated Au atoms.

■ ASSOCIATED CONTENT

Ⓢ Supporting Information

X-ray crystallographic data in CIF format, details of the synthesis, X-ray crystallographic analyses, and supporting figures. This material is available free of charge via the Internet at http://pubs.acs.org.

■ AUTHOR INFORMATION

Corresponding Author

*E-mail: Lai-Sheng_Wang@brown.edu.

Author Contributions

J.C. conceived the synthesis and carried out the experiment along with Q.-F.Z. P.G.W. did the X-ray analyses. L.-S.W. directed the research. J.C., P.G.W., and L.-S.W. wrote the manuscript, and all authors commented on the final version.

Notes

The authors declare no competing financial interest.

■ ACKNOWLEDGMENTS

We thank Prof. W. Bernskoetter for help with the composition analyses. The crystallographic data were obtained through the Service Crystallography at the Advanced Light Source program at the Small-Crystal Crystallography Beamline 11.3.1 at the Advanced Light Source (ALS), Lawrence Berkeley National Laboratory. The ALS is supported by the U.S. Department of Energy, Office of Energy Sciences Materials Sciences Division, under Contract DE-AC02-05CH11231. We are indebted to Dr. Kristyn Roscioli for assistance with high-resolution ESI-MS, which was performed at EMSL, a national scientific user facility sponsored by the Department of Energy's Office of Biological and Environmental Research and located at Pacific Northwest National Laboratory. This work was partially supported through NSF Grant 1058041 (to P.G.W.).

■ REFERENCES

(1) Haruta, M. *Nature* **2005**, *437*, 1098−1099.
(2) Corma, A.; Serna, P. *Science* **2006**, *313*, 332−334.
(3) Hashmi, A. S. K.; Hutchings, G. J. *Angew. Chem., Int. Ed.* **2006**, *45*, 7896−7936.
(4) Jadzinsky, P. D.; Calero, G.; Ackerson, C. J.; Bushnell, D. A.; Kornberg, R. D. *Science* **2007**, *318*, 430−433.
(5) Heaven, M. W.; Dass, A.; White, P. S.; Holt, K. M.; Murray, R. W. *J. Am. Chem. Soc.* **2008**, *130*, 3754−3755.
(6) Zhu, M.; Aikens, C. M.; Hollander, F. J.; Schatz, G. C.; Jin, R. *J. Am. Chem. Soc.* **2008**, *130*, 5883−5885.
(7) Qian, H.; Eckenhoff, W. T.; Zhu, Y.; Pintauer, T.; Jin, R. *J. Am. Chem. Soc.* **2010**, *132*, 8280−828.
(8) Zeng, C.; Qian, H.; Li, T.; Li, G.; Rosi, N. L.; Yoon, B.; Barnett, R. N.; Whetten, R. L.; Landman, U.; Jin, R. *Angew. Chem., Int. Ed.* **2012**, *51*, 13114−13118.
(9) Zeng, C.; Li, T.; Das, A.; Rosi, N. L.; Jin, C. *J. Am. Chem. Soc.* **2013**, *135*, 10011−10013.
(10) Bahena, D.; Bhattarai, N.; Santiago, U.; Tlahuice, A.; Ponce, A.; Bach, S. B. H.; Yoon, B.; Whetten, R. L.; Landman, U.; Jose-Yacaman, M. *J. Phys. Chem. Lett.* **2013**, *4*, 975−981.
(11) Walter, M.; Akola, J.; Lopez-Acevedo, O.; Jadzinsky, P. D.; Calero, G.; Ackerson, C. J.; Whetten, R. L.; Grönbeck, H.; Häkkinen, H. *Proc. Natl. Acad. Sci. U.S.A.* **2008**, *105*, 9157−9162.
(12) Pei, Y.; Gao, Y.; Zeng, X. C. *J. Am. Chem. Soc.* **2008**, *130*, 7830−7832.
(13) Jiang, D. N.; Walter, M.; Akola, J. *J. Phys. Chem. C* **2010**, *114*, 15883−15889.
(14) Pei, Y.; Zeng, X. C. *Nanoscale* **2012**, *4*, 4054−4072.
(15) Jiang, D. E. *Chem.—Eur. J.* **2011**, *17*, 12289−12293.
(16) Heinecke, C. L.; Ni, T. W.; Malola, S.; Makinen, V.; Wong, O. A.; Hakkinen, H.; Ackerson, C. J. *J. Am. Chem. Soc.* **2012**, *134*, 13316−13322.
(17) Maksymovych, P.; Sorescu, D. C.; Yates, J. T. *Phys. Rev. Lett.* **2006**, *97*, 146103.
(18) Hakkinen, H. *Nat. Chem.* **2012**, *4*, 443−455.
(19) Das, A.; Li, T.; Nobusada, K.; Zeng, Q.; Rosi, N. L.; Jin, R. *J. Am. Chem. Soc.* **2012**, *134*, 20286−20289.
(20) Das, A.; Li, T.; Nobusada, K.; Zeng, C.; Rosi, N. L.; Jing, R. *J. Am. Chem. Soc.* **2013**, *135*, 18264−18267.
(21) McPartlin, M.; Mason, R.; Malatesta, L. *J. Chem. Soc., Chem. Commun.* **1969**, *7*, 334−334.
(22) Amasser, M.; Naldini, L.; Sansoni, M. *J. Chem. Soc., Chem. Commun.* **1979**, *9*, 385−386.
(23) Smits, J. M. M.; Bour, J. J.; Vollenbroek, F. A.; Beurskens, P. T. *J. Crystallogr. Spectrosc. Res.* **1983**, *13*, 355−363.
(24) Briant, C. E.; Theobald, B. R. C.; White, J. W.; Bell, L. K.; Mingos, D. M. P.; Welch, A. J. *J. Chem. Soc., Chem. Commun.* **1981**, *5*, 201−202.
(25) Hall, K. P.; Mingos, D. M. P. *Prog. Inorg. Chem.* **1985**, 237−325.
(26) Shichibu, Y.; Kamei, Y.; Konishi, K. *Chem. Commun.* **2012**, *48*, 7559−7561.
(27) Shichibu, Y.; Suzuki, K.; Konishi, K. *Nanoscale* **2012**, *4*, 4125−4129.
(28) Wan, X. K.; Lin, Z. W.; Wang, Q. M. *J. Am. Chem. Soc.* **2012**, *134*, 14750−14752.
(29) Gutrath, B. S.; Oppel, I. M.; Presly, O.; Beljakov, I.; Meded, V.; Wenzel, W.; Simon, U. *Angew. Chem., Int. Ed.* **2013**, *52*, 3529−3532.
(30) Yanagimoto, Y.; Negishi, Y.; Fujihara, H.; Tsukuda, T. *J. Phys. Chem. B* **2006**, *110*, 11611−11614.
(31) Shichibu, Y.; Konishi, K. *Small* **2010**, *6*, 1216−1220.
(32) Li, J.; Li, X.; Zhai, H. J.; Wang, L. S. *Science* **2003**, *299*, 864−867.
(33) Zhang, H. F.; Stender, M.; Zhang, R.; Wang, C.; Li, J.; Wang, L. S. *J. Phys. Chem. B* **2004**, *108*, 12259−12263.
(34) Bertino, M. F.; Sun, Z. M.; Zhang, R.; Wang, L. S. *J. Phys. Chem. B* **2006**, *110*, 21416−21418.
(35) Chen, J.; Zhang, Q. F.; Bonaccorso, T. A.; Williard, P. G.; Wang, L. S. *J. Am. Chem. Soc.* **2014**, *136*, 92−95.
(36) Balch, A. L.; Fung, E. Y. *Inorg. Chem.* **1990**, *29*, 4764−4768.
(37) Typical synthetic procedures and crystal structure details are provided in the SI. CCDC 985958 contains the supplementary crystallographic data for this paper. See the supporting CIF file.
(38) Mingos, D. M. P. *Chem. Soc. Rev.* **1986**, *15*, 31−61.
(39) Pyykko, P. *Angew. Chem., Int. Ed.* **2004**, *43*, 4412−4456.